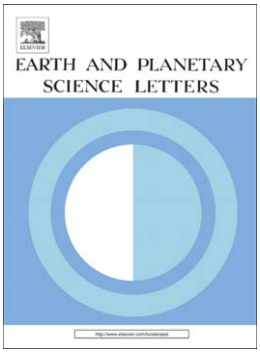

Quenching of steam-charged pumice: Implications for submarine pyroclastic volcanism

S.R. Allen, R.S. Fiske, K.V. Cashman

PII: S0012-821X(08)00421-4
DOI: doi: 10.1016/j.epsl.2008.06.050
Reference: EPSL 9389

To appear in: *Earth and Planetary Science Letters*

Received date: 19 February 2008
Revised date: 23 June 2008
Accepted date: 29 June 2008

Please cite this article as: S.R. Allen, R.S. Fiske, K.V. Cashman, Quenching of steam-charged pumice: Implications for submarine pyroclastic volcanism, *Earth and Planetary Science Letters* (2008), doi: 10.1016/j.epsl.2008.06.050

Quenching of steam-charged pumice: Implications for submarine pyroclastic volcanism

S.R. Allen[a,*], R.S. Fiske[b], K.V. Cashman[c]

[a]School of Earth Sciences and Centre of Excellence in Ore Deposits, University of Tasmania, Private Bag 79, Hobart, Tasmania 7001, Australia, Sharon.Allen@utas.edu.au

[b]Smithsonian Institution MRC-119, Washington, DC 20560, USA, fisker@si.edu

[c]Department of Geological Sciences, University of Oregon, Eugene, OR 97403-1272, USA, cashman@uoregon.edu

* Corresponding author: Tel.: +61 3 62267635; fax: +61 3 6226 7662.
E-mail address: Sharon.Allen@utas.edu.au

Abstract

Huge quantities of silicic pumice have been deposited in intra-oceanic convergent margin settings throughout Earth's history. The association of submarine silicic calderas with thick proximal accumulations of pumice lapilli suggests that these pyroclasts were deposited as a direct result of submarine eruptions. Yet when first erupted, these highly vesicular, gas-filled clasts had densities significantly less than seawater. Experiments carried out 1-atm on heated pumice samples whose vesicles were charged with steam, the dominant component of magmatic volatiles show that buoyancy of freshly erupted submarine pumice is transient. Upon quenching, the phase change of steam to liquid water creates strong negative pore pressures within the pumice vesicles that accelerate the absorption of surrounding water, generating high-density pumice and promoting rapid clast sinking. Variations in the physical properties of steam with temperature and pressure have important implications for submarine pyroclastic eruptions. Firstly, highly vesicular pumice can be deposited on the seafloor at temperatures elevated significantly above ambient if they are erupted at sufficient depths to remain wholly submarine (>~200 m) and either the fluid in which they cool contains heated water and/or they only absorb sufficient water to sink. Secondly, the rapid increase in density of the eruption column caused by condensation and the transition from buoyant (gas-filled) to denser (water-saturated) pumice lapilli, together with turbulent mixing with the surrounding seawater favour collapse and transport of pyroclasts in water-supported gravity currents. Finally, this mixing of the ejecta with seawater and the ease of water ingestion into permeable pumice clasts suggest that water-supported transport mechanisms can operate as primary dispersal processes in explosive submarine eruptions.

Keywords: submarine pumice, steam condensation, submarine pyroclastic eruption, quenching, welding.

1. Introduction

Pumice is highly vesicular volcanic glass formed during eruptions of water-rich silicic magma. When the vesicles in pumice are filled with gas, these clasts are buoyant in water. Historic emergent and ocean-island silicic eruptions have generated extensive rafts of floating pumice that were widely dispersed, such as those that followed the August 2006 eruption at Home Reef submarine volcano (Smithsonian Institution, 2006) and the 1883 eruption of Krakatau (Simkin and Fiske, 1983). Yet exploration of present-day submarine arcs shows that aprons of pumice surround submarine explosive calderas (e.g., Izu-Bonin arc, Nishimura et al., 1991; Fiske et al., 2001; Kermadec arc, Wright et al., 2003, Wright et al., 2006). Uplifted successions of modern submarine arcs also attest to the pumice-rich nature of the deposits (e.g., Hellenic arc, Allen and McPhie, 2000; Rinaldi and Campos Venuti, 2003; Stewart and McPhie, 2004, 2006), as do thick seafloor pumice deposits in marine sedimentary sequences associated with ancient volcanic arcs (e.g., Cambrian Mount Read Volcanics, Australia, McPhie and Allen, 2003; Mesozoic Mineral King pendant, California, Busby-Spera, 1984; Miocene Green-Tuff Belt, Japan, Fiske and Matsuda, 1964). These submarine pumice deposits are highly prospective, as many host VHMS (volcanic-hosted massive sulfide) ore bodies (e.g., Morton et al., 1991; Gibson et al., 1999; Iizasa et al., 1999; Hudak et al. 2003). The common occurrence of pumice in the marine record raises important questions about the origin of these deposits. In particular, because pumice is known to float, its occurrence in large volumes on the seafloor must be explained.

To address this problem, we investigate water ingestion by hot pumice clasts having variable pore structures (porosity and permeability) and differing proportions of steam and liquid water in their vesicles. These experiments demonstrate that the influx of water into steam-charged pumice is rapid during quenching. Extrapolation of our findings to pressures appropriate for magmatic-volatile-driven explosive eruptions in deep water suggests that: (1) at least the quenched margins of submarine eruption columns can transform rapidly from buoyant to collapsing, the latter generating water-supported, pyroclastic density currents; (2) both the clast cooling history (related to pumice size) and internal pumice structure (permeability) will influence whether a single pumice clast is deposited by settling through the water column or from collapse-generated submarine gravity currents; and (3) the emplacement temperature is influenced by the depth at

77 which the clast becomes water saturated and porosity of the pumice. Our work on steam-
78 charged pumice extends and expands the experimental work of Whitham and Sparks
79 (1986) and Dufek et al. (2007) on the interaction of subaerial (air-filled) pumice with
80 seawater to the submarine environment, providing a quantitative framework for eruptive
81 and depositional processes in intra-oceanic convergent margin settings.
82
83 *1.1 Background and previous work*
84
85 The discovery of pumice clasts in ancient marine volcanic successions now uplifted onto
86 land, and the concept that some of these pumice lapilli tuffs were derived directly from
87 submarine explosive eruptions, were highlighted in the pioneering work of RS Fiske
88 (Fiske, 1963; Fiske and Matsuda, 1964; Fiske 1969). Since that time, several submarine
89 calderas formed by explosive eruptions of silicic magma and their infilling syn-caldera
90 pumice deposits have been interpreted in ancient successions (e.g., De Rosen-Spence et
91 al., 1980; Busby-Spera, 1984; Hudak et al., 2003). It is only recently, however, that
92 seismic profiles and submarine bathymetric data have confirmed the presence of calderas
93 on the modern seafloor (e.g., Izu-Bonin arc, Murakami and Ishihara, 1985; Yuasa et al.,
94 1991; Yuasa and Kano, 2003; Kermadec arc, Wright and Gamble, 1999; Wright et al.,
95 2006; Mariana Arc, Stern et al., 2008). Dedicated submersible and/or remotely operated
96 vehicle dives on Myojin Knoll caldera (Fiske et al., 2001), Sumisu caldera (Tani et al.,
97 2008) and West Rota Volcano (Stern et al., 2003), and dredge-sampling on Healy caldera
98 (Wright et al., 2003) have shown that these calderas have produced substantial volumes
99 of highly vesicular pumice deposits on the seafloor. In particular, the eruption that
100 produced the Sumisu caldera is considered to be the source of the thick, pumice lapilli-
101 tuffs that were discovered during ODP drilling in the Sumisu rift basin, 70 km away
102 (Nishimura et al., 1991, Tani et al., 2008).
103 The lithofacies characteristics of well preserved, uplifted Miocene to Recent
104 eruption-fed, submarine pyroclastic pumice deposits include, (1) double grading, where
105 each bed is density graded, and the bedsets are normally graded overall (Fiske and
106 Matsuda, 1964), (2) hydraulic sorting (Cashman and Fiske, 1991), and (3) well-defined
107 organisation into lithic-rich bases, pumice lapilli-rich main parts, and upper pumice block

and/or ash facies (Kano et al., 1996; Allen and McPhie, 2000; Stewart and McPhie, 2004). Such features indicate that the transport and depositional dynamics of the erupted ejecta are strongly influenced by cooling and mixing with the surrounding seawater. Theoretical considerations of the eruption dynamics have focussed on the effects of this turbulent mixing on column stability, leading to the conclusion that the ejecta from submarine eruptions quickly become negatively buoyant and collapse (Kano et al., 1996; Head and Wilson 2003). Recent review papers on subaqueous eruption-fed density currents and their deposits (White 2000), historic submarine pumice eruptions (Kano 2003), and explosive submarine eruptions (White et al., 2003), discuss the processes by which pumice can be erupted and deposited on the seafloor, including the role of magmatic gases and external steam production on plume behaviour.

Moreover, understanding of the mechanisms that cause submarine-erupted low-density pumice lapilli to sink has been heavily dependent on the experimental study of Whitham and Sparks (1986), who addressed a different problem, that is, the behaviour of hot subaerially erupted pumice that enters the ocean in pyroclastic density currents. Whitham and Sparks (1986) heated air-filled, highly vesicular pumice (densities 200-300 kg/m^3) before forcing them under water. When heated to temperatures $\geq 400^oC$, these air-filled clasts absorbed water and sank by a two step process: firstly, air was flushed out of the vesicles by steam generated from the interaction of the hot clast with water. Secondly, ingestion of water resulted from contraction and condensation of the steam. Pumice at lower temperatures ($<300^oC$) was much less efficient at generating steam and therefore remained sufficiently air-filled to float. For this reason, it has been generally assumed that only hot ($\geq 400°$ C) pumice can sink efficiently in water.

Interpretations based on these experiments may be less applicable to the behaviour of pumice produced in submarine environments, where vesicles are filled with magmatic gases (mostly steam) rather than air. Nitrogen and oxygen, the chief components of air, are not magmatic gases, and in contrast to steam, do not undergo a phase change while cooling through temperature ranges encountered by submarine eruptions. Condensation of steam causes a dramatic change in volume creating negative pore pressures that accelerate ingestion of the surrounded seawater fluid (e.g., Kato, 1987; Kano et al., 1996; Cashman and Fiske, 1991; Fiske et al., 2001). To test the efficiency of this mechanism, we have

performed a series of 1 atm experiments on steam-charged rhyolitic pumice samples that were initially fully water-saturated. The physics of steam condensation is universal regardless of the pressure conditions, hence, results of quenching experiments undertaken at atmospheric pressure can be realistically extrapolated to higher pressure conditions below the critical point.

2. Steam experiments

2.1 Sample properties

Four blocks of unaltered, fully water-saturated rhyolitic pumice were collected from thick, coarse unconsolidated pumice breccias on the seafloor at depths of 1470-320 m in the Izu-Bonin arc and back arc by Remotely Operated Vehicle (ROV) and dredging during JAMSTEC research cruises KV04-04 and NT04-10 (Table 1). As these clasts are fresh (unaltered and without manganese crusts), large (>30 cm across), and contain relatively homogeneous vesicle populations, their textures are similar in the multiple 2 cm-cubes that were cut. Seawater was flushed out and replaced by fresh water by suction. The water-saturated pumice cubes were individually numbered and weighed while suspended in water [m_{sat}(water)] (dabbed for ~2 seconds on moist chamois to remove excess water), and then weighed again in air [m_{sat}(air)]. Water saturated specific gravities were calculated as:

$$S.G._{sat} = m_{sat}(air)/[m_{sat}(air) - m_{sat}(water)]$$

The variation in water saturated S.G. due to vesicle heterogeneities within each block was less than 5% (Table 1, Fig. 1). On completion of the steam experiments, the cubes were furnace dried (1-2 hr at 200-400C°) and weighed to calculate their specific gravity when dry, where

$$S.G._{dry} = m_{dry}(air)/[m_{sat}(air) - m_{sat}(water)]$$

Dense-rock S.G. for each pumice clast were measured by He-pycnometer using powdered samples. Theoretical water-saturated S.G. were calculated for each cube, where

$$S.G._{sat}\ (\text{theoretical}) = 1 + S.G._{dry} - (S.G._{dry}/S.G._{\text{dense rock}})$$

Variations in measured water-saturated S.G. from theoretical values were <3% and attributed to leakage from large pores during weight-in-air measurements (Table 1, Fig. 1). Bulk and connected porosities and abundances of isolated vesicles of dry (air-filled) samples were measured by He-pycnometer following the method of Klug and Cashman (1996). We also measured the permeability of 25 mm-diameter cores cut from the pumice clasts with a permeameter/porometer following the method of Rust and Cashman (2004).

2.1 Experimental method

The experiments were designed to measure the effects of steam condensation on the uptake of water during quenching of pumice clasts. They involved two stages: (1) Steam experiments, where the fully water-saturated cubes were heated in a furnace at a set temperature so that a fraction of the pore water was replaced with steam. At the desired water/steam ratio, the cubes were quenched in room-temperature (21^{o}) water and reweighed to determine the efficiency of water absorption. (2) Air experiments where the same pumice cubes were then dried, heated to the same temperature as the steam run, quenched, and reweighed to determine the efficiency of water resorption in the cube in the absence of interstitial steam.

At 1 atm the phase change from steam to liquid water occurs at 100^{o}C, so that experiments to measure the effects of steam condensation were undertaken at temperatures elevated slightly above 100^{o}C (110 , 125 and 150^{o}C). To distinguish the effects of steam condensation from capillary action and gas contraction, the steam experiments included runs at higher temperatures (200 to 500^{o}C). Air experiments were performed at temperatures that ranged between 21 ^{o}C and 500^{o}C.

Steam experiments:

1) Initially, samples from each pumice clast were furnace dried to permit calculation of their dry specific gravities. Then for each cube used in the steam experiments, the approximate mass could be calculated to reflect the desired steam/water ratio prior to quenching. Steam/water ratios were chosen at 30/70, 50/50 and 70/30 to reflect stages in water ingestion in a theoretically cooling pumice clast. Ratios were chosen to reduce the proportion of water sufficiently to make the cube initially buoyant (≤70%), but with minimum contamination of air (≥30%). The cubes were tightly wrapped in aluminium-foil to further reduce contamination with air.

2) Experimental runs were conducted at furnace temperatures of 110°C, 125°C, 150°C, 200°C, 300°C, 400°C and 500°C. A total of 12 cubes were used for each temperature run - three cubes from each pumice block; one at each steam/water ratio. Because the experiments were designed to retain some liquid water in the cube, each cube experienced a temperature gradient that ranged from below 100°C in the cube interior to the furnace temperature towards the cube margin.

3) As each cube was heated, the interstitial water boiled and was progressively transformed to steam. The mass of water-loss for each cube was measured periodically by rapid (5 sec round trip) removal and weighing on an adjacent top-loading balance. The rate of water loss was plotted to predict the time when the desired steam/water ratio would be reached (Fig. 2a).

4) At the desired steam/water ratio, the steamy cube was quenched by plunging into 21°C water; the Al-foil was quickly removed while being held under water. After a set time interval (5 minutes was chosen to allow the clast to fully cool and reach an equilibrium saturation), the cube was removed from water, dabbed for ~2 seconds on moist chamois, and weighed to determine the resaturation mass.

5) The cubes were then dried and weighed dry to permit calculation of their dry specific gravities and determine their actual steam/water ratio on quenching.

Air experiments:

6) Each (Al-clad) dried cube was reheated to the same temperature as its water-saturated run, with additional temperature runs of 21°C and 70°C. The air-filled cube was then

weighed and quenched in water following the procedure for the steam-charged cubes to determine the comparative re-saturation mass.

7) As a control, 12 dry cubes (the same 3 cubes selected from each pumice clast) were heated, quenched and weighed for saturation after quenching at each of the temperature runs. These experiments tested the variability in saturation on quenching of the same clast when heated to different temperatures (Fig. 2b).

3. Results and interpretation

The primary goal of our experiments was to determine controls on the efficiency of water resorption by pumice clasts when immersed in water. In all experiments, we define the efficiency of water absorption as the extent to which a pumice cube re-saturates after heating, quenching and immersion in water for 5 minutes compared to its fully water-saturated, pre-experiment mass. The absorption factor (α) was defined as $\alpha = (m_{resaturated} - m_{air\text{-}filled})/(m_{saturated} - m_{air\text{-}filled})$ where m is the mass of the cube; α can therefore vary between 0 (no resorption) and 1 (fully resorption; Fig. 3).

3.1 Water and steam-filled pumice

When heated above the liquid water-steam transition (100^{o}C at 1-atm), all steam-charged pumice cubes sank quickly when quenched regardless of their pre-quench temperature, re-absorbing most of the water temporarily displaced by steam (Fig. 3). Ideally, the uptake of water due to steam condensation in the pore spaces during quenching should have returned all cubes to full saturation (absorption factors of 1). However, saturation was commonly less than 100% and varied predictably with pre-quenching conditions. Pumice cubes having the highest pre-quench water/steam ratios (70/30; red dots) had the highest re-absorption factors ($\alpha \geq 0.95$). All but two of those having 50/50 water/steam ratios had $\alpha \geq 0.90$ (blue dots), and only one of those having 30/70 ratios (green dots) had $\alpha < 0.8$. In the latter two sets of experiments, α increased with increasing pre-quench temperature. We have identified two sources of experimental error that probably

contributed to less than perfect water resorption; differences in resorption potential generated by details of the pore structure are discussed later.

(1) *Air contamination*. Our experiments did not prevent the loss of steam from the cubes, and resulting contamination by air, during the repeated out-and-into-furnace weighings because of leakage through the aluminium foil wrap enclosing each cube. The data points representing steam/water ratios of 30/70 (red), 50/50 (blue), and 70/30 (green) (Fig. 3), show progressive decreasing re-absorption factors, indicating that errors were greater with increasing time in the furnace and increasing numbers of weighing cycles.

(2) *Weighing error*. Measurement of pumice mass (both saturated and re-saturated) generated errors of ≤2%. Greater errors were associated with samples containing larger coalesced vesicles because of rapid water drainage from vesicles.

3.2 Air-filled pumice

Absorption characteristics of the air-filled pumice cubes differ markedly from the steam-charged cubes (open circles; Fig. 3). Between 21°C and ~300°C, α of air-filled cubes increase as temperature increases. Above 300°C, less vesicular cubes (337-1, 339-8; 73 vol% vesicles; Figs. 3c, 3d) are almost completely water-saturated whereas cubes with higher vesicularities (D7, 337-5; 80 vol% vesicles; Figs. 3a, 3b) fail to reach complete water-saturation, even at temperatures of 500°C.

At room temperature (21°C), where there is no temperature change on immersion in water, absorption may occur by capillary forces (related to pressure and surface tension); our data suggest that capillarity can account for absorption factors of ~ 0.4 (capillary+ field; Fig. 3a). With increasing initial temperature, absorption is enhanced by cooling contraction of the air within the vesicles. According to the ideal gas law (assuming that pressure and mole fraction of air remain constant):

$$V_1 / V_2 = T_1 / T_2,$$

where V_1 and V_2 and T_1 and T_2 are volumes and temperatures (in Kelvin) after heating (just before quenching) and on quenching to ambient temperatures. For example, on

quenching from temperatures of 573K (300°C), air contracts to about half its volume, giving an absorption factor of ~0.5 ($1-T_2/T_1$ contraction field; Fig. 3a). At temperatures ≥400°C (673K), the absorption process is overshadowed by the phase change of steam (steam field; Fig. 3a) generated from the interaction of the hot glass with water (e.g., Whitham and Sparks, 1986; Dufek et al., 2007).

3.3 Behaviour of air- versus steam-charged hot pumice

The differences in absorption efficiency between air-filled and steam-charged pumice illustrate the importance of the volatile phase composition on quenching behaviour. Steam-charged pumice ingests water rapidly, reaching essentially full saturation as soon as the steam condenses (at the steam-liquid water phase transition temperature) and sinks (grey field in Fig. 3). In contrast, air-filled pumice partially saturates to a degree that depends on the initial temperature and vesicularity. For this reason, the largest differences in α between steam-charged and air-filled pumice occurs at the lowest temperatures (<300°C), where the steam generated is not sufficient to cause saturation of pumice clasts on quenching and water ingestion occurs by cooling contraction of air and capillary action (e.g., Whitham and Sparks, 1986).

As noted by Whitham and Sparks (1986), the initial vesicularity of hot air-filled pumice clasts dictates the absorption factor required for the clast density to exceed that of seawater. This relationship is illustrated by comparing air-filled clasts with 80% vesicles, which sank at $T > 300^{\circ}C$ ($\alpha \geq 0.7$; Figs. 3a, 3b) with those with 73% vesicles, which sank at $T > 125^{\circ}C$ ($\alpha \geq 0.58$; Fig. 3c, 3d). This vesicularity dependence is not observed in steam-charged pumice, where all clasts had $\alpha >> 0.7$ and therefore sank as soon as the steam-liquid water phase transition was reached.

Our results thus show that pumice can absorb water and sink at the steam-liquid water phase change temperature if the vesicles are initially charged with steam. Moreover, cooling from temperatures far above this phase transition does not further increase the absorption efficiency, in contrast to the strong dependence of sinking efficiency on the temperature of air-filled clasts. Finally, air-filled clasts never achieved full saturation, although all clasts sank when heated to sufficiently high temperatures.

322 Thus we expect pumice cooled from magmatic temperatures and flushed by air prior to
323 contact with water to have very different water-ingestion capabilities than submarine-
324 erupted pumice filled with H_2O-rich magmatic gases that never reaches sea level.
325
326 *3.4 Influence of pore structure on water absorption*
327
328 Our experiments suggest that textural variations in the seafloor pumice blocks
329 influenced the absorption characteristics of the cubes sawn from them. To assess the
330 importance of pore structure on α, we measured the connected porosity, isolated porosity,
331 and permeability of all analysed samples. All pumice clasts are highly vesicular (73-80
332 vol% vesicles); these vesicles are mostly (>97%) connected. Both the high porosities and
333 high degree of interconnectivity lead to high clast permeabilities ($2.5 – 10 \times 10^{-12}$ m^2). In
334 detail, sample D7 exhibits both high vesicularities and uniform vesicle geometries,
335 resulting in both high permeability (9.9×10^{-12} m^2; Table 1) and high water absorption
336 efficiency of this sample ($T < 200^{\circ}C$, $\alpha \geq 0.87$; Fig. 3a). The other three pumice samples
337 comprise both elongate and round coalesced vesicle domains and/or display a greater
338 range in vesicle size (up to 5 mm) and lower permeabilities ($2.4\text{-}3.2 \times 10^{-12}$ m^2). As a
339 result, these cubes have slightly lower absorption efficiencies ($T < 200^{\circ}C$, $\alpha \geq 0.74$) than
340 the D7 cubes, particularly as the phase change temperature is approached.
341
342 *3.5 Submarine-erupted pumice properties*
343
344 The pumice blocks used in the experiments have vesicularities and permeabilities typical
345 of submarine erupted and deposited pumice clasts collected from knolls on the modern
346 sea floor of the Izu-Bonin Arc, Japan and from uplifted successions in the Aegean Arc,
347 Greece (Fig. 4). Our suite of over 200, highly vesicular, silicic pyroclastic and quenched-
348 dome margin samples, have typical vesicularities of 60-80 vol%, permeabilities of $>10^{-13}$
349 m^2 and are dominated by connected vesicles (>90 vol%). These high permeability and
350 vesicularity ranges appear typical of silicic pumice regardless of whether they were
351 erupted in the submarine or subaerial environment (cf. Klug and Cashman, 1996). Such

high permeabilities are equivalent to those of well-sorted sands and glacial outwash, although the porosities of sediments are much lower (25-50 vol%; Fetter 1988).

There are however two unusual characteristics of submarine erupted and deposited pumice that affect clast dispersal characteristics. Firstly, a feature that was first recognised by Fiske (1969) in ancient submarine successions is that much of the pumice is the long-tube variety. The vesicles have a dominant elongation direction, and range from elongate to being highly attenuated (Fig. 5a). In these clasts, permeabilities can vary by up to 4 orders of magnitude depending on the orientation of the measurement; important for settling properties is the very high permeability measured parallel to vesicle elongation. In contrast, submarine-erupted pumice clasts with a high percentage of spherical and isolated vesicles tend to float for long periods of time (Fiske, 1969), and are thus washed up at coastlines or deposited from floating rafts at substantial distances from source. For example Kato (1987) found that pumice that remained floating from the submarine eruption off Iriomote Island in 1924 had very high proportions (37 vol%) of isolated vesicles. Saturation of pumice with spherical vesicles is governed by capillary pressure required for water to move through the very small pores formed during partial vesicle coalescence (Klug and Cashman, 1996). Secondly, there is a tendency for coarse lapilli and larger clasts to fracture as a result of quenching in water. Fracturing is manifested as intensely shattered to jointed (at a cm-scale) margins and polyhedral or curviplanar internal fracture surfaces (Fig. 5b). The effect of this process is illustrated by large m-sized pumice blocks that rose to the surface from the 1934-1935 deep submarine eruptions of Shin-Iwojima, Japan (Kano et al., 2003) and floated only briefly while steaming and cracking before sinking. Thus, fracture-controlled permeability appears to allow effective and rapid saturation of large hot pumice clasts.

4. Implications for submarine pyroclastic eruptions

Magmatic-volatile-driven explosive eruptions are triggered by overpressures related to the decompression of volatiles in the magma (McBirney, 1963; Wilson et al., 1980) which drives the ejecta upwards at high exit velocities. In subaerial eruptions, further ascent occurs as a result of mixing of this turbulent jet with air, which considerably

lowers the density of the ejecta and generates a buoyant plume. Subaqueous pyroclastic eruptions however, are expected to behave differently from their subaerial counterparts. For example, the pressure exerted by the overlying water column retards volatile exsolution, vesiculation and decompression-driven exit velocities; the high heat capacity and thermal conductivity of water accelerates cooling; and, the greater viscosity and density of seawater relative to air affects buoyancy and patterns of clast transport (Cashman and Fiske, 1991; Kokelaar and Busby, 1992; Kano et al., 1996; Head and Wilson, 2003; White et al., 2003; Stewart and McPhie, 2004).

Quantitative analysis of the behaviour of submarine pyroclastic eruptions predicts that the jet mixes extensively with water through turbulence (Head and Wilson, 2003). The thermal diffusivity of steam varies with temperature and pressure (2 x 10^{-5} m^2/s for steam at 100^{o}C and 0.1 MPa; 2 x 10-6 m^2/s for steam at 180^{o}C at 1 MPa), but is significantly higher than that of pumice (~2.5 x 10^{-7} m^2/s). Hence, the inter-particle steam will rapidly cool and condense, accelerating the mixing of the ejecta with seawater due to negative pressures created during condensation. This change in plume composition from gas-dominated to water-dominated is therefore likely to occur quickly, at least at the margins of the jet. Furthermore, Head and Wilson (2003) predict that this cooling and mixing with water will cause the jet to collapse and segregate from the ash, which will be elutriated to form a plume. However, Head and Wilson (2003) did not trace fate of ejecta dominated by highly vesicular pumice clasts. Here we explore the ramifications of the steam-liquid water phase change on the behaviour and depositional processes accompanying submarine explosive eruptions where pumice is the dominant clast type.

4.1 Transient buoyancy

On eruption, vesicles in the pumice clasts are filled with magmatic gases and rise through the water column as a result of the combined effects of initial eruption flux and buoyancy. However, steam, the dominant component of magmatic gas, which has a low density and high buoyancy, condenses to higher density liquid water once it cools through the phase-change temperature, drawing in the surrounding water. Theoretically, on cooling, pumice clasts will begin to fill with seawater, gradually at first because of the

414 combined effects of capillary forces and the volume change of magmatic gases due to
415 contraction and then abruptly because of the condensation of magmatic steam. For
416 example, in order to sink, pumice with 60 vol% vesicles needs only 10% of the vesicles
417 to be water-saturated whereas clasts with 85 vol% vesicles requires saturation of 75% of
418 the vesicles (Figs. 6, 7). Therefore, in order for pumice clasts to remain buoyant, they
419 must be sufficiently hot to remain steam-filled (Cashman and Fiske, 1991; Kano et al.,
420 1996; Fiske et al., 2001). The rate of cooling of pumice is also dependent on clast size,
421 and larger clasts cool more slowly because of their greater thermal mass (Thomas and
422 Sparks, 1992; Kano et al., 1996). Kano et al. (1996) used equations of Carslaw and Jaeger
423 (1959) to calculate times required for complete cooling of pumice clasts to condensation
424 temperatures for different clast sizes. These calculations give maximum cooling rates
425 from conductive cooling. The results suggest that cooling the clast interiors to 180^{o}C, the
426 phase change temperature at 1 MPa (100 mbsl), for coarse ash (≤ 2 mm), fine lapilli (≤ 16
427 mm) and coarse lapilli (≤ 64 mm) would take no longer than 1.6 seconds, 1.7 minutes
428 and 27 minutes, respectively. These calculations led Kano et al. (1996) to suggest that
429 smaller pumice clasts cool on contact with water and become water-logged. As the
430 behaviour of eruption columns is sensitive to density changes, the cooling and mixing of
431 the ejecta with seawater together with the dramatic increase in density of pumice lapilli
432 during cooling is predicted to destabilize the column, promoting collapse, and initiating
433 transport of negatively buoyant pyroclasts in water-supported gravity currents, essentially
434 conforming with the model of Head and Wilson (2003). Therefore, pumice lapilli that
435 cool and absorb water more readily than larger clasts, will be over-represented in deposits
436 resulting from collapse-generated flows. Such pumice lapilli-rich flow deposits have
437 been reported in field studies of uplifted successions in Japan and Greece (e.g., Shinjima
438 pumice, Kano et al., 1996; Yali pumice, Allen and McPhie, 2000; Filakopi pumice unit
439 B, Stewart and McPhie, 2004) (Fig. 5c).
440 In contrast, coarse lapilli and blocks that remain sufficiently hot to be buoyant,
441 rise out of the collapsing fountain in thermal convecting plumes of heated water (e.g.
442 Kano et al., 1996). We suggest that, for these large buoyant clasts, magmatic steam and
443 other gases filling vesicles at depth will continue to decompress, acting to accelerate their
444 rise rate and inhibit contact with the surrounding water. Once these large clasts reach the

surface and decompression is complete, they begin to cool. Hot pumice clasts were observed to billow steam as they floated on the sea surface during the 1934 eruption at Shin-Iwojima, south of Kyushu, Japan (Kano, 2003) and the 1953-1957 eruption of Tuluman volcano, northern Bismarck Sea (Reynolds et al., 1980). In this low-pressure environment, the steam to liquid water phase change is accompanied by a 1600-fold volume decrease, and thermal-contraction fractures that form in the pumice, accelerate the ingestion of water into the clast. Hence, these fractured clasts quickly begin to saturate and sink. While doing so, any remaining gas in the vesicles continues to contract while settling through the increasing pressures in the water column, causing settling velocities to increase. For example, large pumice blocks (10-100+ cm) within the Yali pumice cobble-boulder facies (Allen and McPhie, 2000) and Filakopi pumice unit C (Stewart and McPhie, 2004) (Fig. 5d), are interpreted to have separated from the collapsing column and ascended buoyantly to the sea surface before settling to the seafloor and are deposited after the collapse generated deposits. Deposits derived from quenched, submarine pumice eruption columns therefore tend to show an overall reverse grading in pumice clast size from lapilli (base) to blocks (upper part), reflecting differing cooling rates and transport mechanisms.

In addition, dense conduit- and vent-derived lithic clasts are too heavy to be entrained in the jet and, fall out rapidly to form basal lithic breccias (Stewart and McPhie, 2004). Furthermore, fine ash particles, having low settling velocities, are readily elutriated during eruption and transport and can be transported many kilometres from the eruption site as water-settled fallout or in sufficient concentrations form ash-rich density currents. Many submarine-erupted pumice deposits are therefore fines-poor (e.g., Fiske, 1963; Fiske and Matsuda, 1964; Fiske, 1969; Kano et al., 1996; Allen and McPhie, 2000; Stewart and McPhie, 2004).

The patterns of pyroclast transport and deposition outlined above also differ from those resulting from subaerial eruptions that enter the sea. In this environment, pumice lapilli cool in air, ingests air, and falls to the sea surface with their vesicles filled with air. Large proportions of these pumice lapilli float and can be rafted far from the eruption site (e.g., Simkin and Fiske, 1983; Bryan et al., 2004). In contrast, negatively buoyant clasts

475 settle through the water column generating submarine deposits that are rich in dense lithic
476 clasts.
477 Our findings reinforce the concept first proposed by Fiske and Matsuda (1964),
478 that the direct products of explosive submarine eruptions can form primary seafloor
479 pyroclastic deposits. However, these submarine eruption-fed deposits differ markedly in
480 facies characteristics from their subaerial counterparts.
481
482 *4.2 Effect of increasing water depth*
483
484 A major challenge to understanding submarine eruptions is determining the effect of
485 increasing water depth (pressure) on the style of eruptive activity. The reduction in water
486 exsolved from the magma with pressure controls the volatiles available to drive explosive
487 submarine eruptions (McBirney, 1963). Using the model of Wilson et al., (1980), we
488 calculate that for rhyolites with magmatic water contents of 5-7 wt%, exit velocities will
489 be reduced by ~1/2 at 500 m water depth, and by ~1/4 at 1000 m water depth because of
490 variations in water solubility, alone. In addition, Head and Wilson (2003) predict that
491 although the density of the ejecta increases with water depth, less thermal energy is lost
492 during mixing with ambient seawater and hence lower but hotter fountain mixtures are
493 generated. Several weakly vesiculated rhyolites in ancient successions have been
494 interpreted to be sourced from these deep-water dense fountains (e.g., Kokelaar and
495 Busby, 1992; Mueller and White, 1992; Busby, 2005).
496 Submarine eruptions that generate highly vesicular pumice at a few hundred meters
497 water depth are fairly common, as indicated by both vent depth estimates for well
498 exposed uplifted submarine pyroclastic pumice deposits (e.g., Fiske and Matsuda, 1964;
499 Kano et al., 1996; Allen and McPhie, 2000; Stewart and McPhie, 2004) and historic
500 pumice-forming submarine eruptions (Kano, 2003). The submarine caldera-forming
501 eruption that deposited the Shinjima Pumice was sourced in as little as 200 m of water,
502 indicating that this depth was sufficient to suppress jet heights and cause column collapse
503 (Kano et al. 1996). While studies of calderas on the modern seafloor suggest that
504 magmatic volatile-driven eruptions generating highly vesicular pumice have occurred at
505 depths of 500 m and possibly as much as 1000 m (Fiske et al., 2001; Wright et al., 2003,

Yuasa and Kano, 2003; Wright et al., 2006). At a depth of 200 m (2 MPa) the steam-liquid water phase transition temperature is 212°C, more than 100˚C greater than at sea level, and at 500-1000 m the phase transition is in the range 260-310˚C. What is the effect of such elevated temperatures on pumice erupted and deposited at these depths?

4.3 Hot submarine pumice deposits?

As the critical point of H_2O is approached, the density change across the steam-to-liquid water phase transition decreases, and the temperature increases. Although unlikely to have a major effect on the process of magmatic vesiculation, which typically occurs at much higher temperatures and pressures, changes in the physical properties of steam will affect post-eruptive interaction of pumice with seawater. The cooling interval over which submarine-erupted pumice exceeds the density of seawater and begins to sink depends on vesicularity and ambient pressure, which determine the steam volume and temperature of the steam-liquid water phase transition.

Theoretically, pumice clasts can remain substantially above 100°C and still sink (Fig. 6). Our experiments show that sufficient water is ingested in clasts that have less than ~ 80 vol% during cooling to initiate sinking, even above the phase transition temperature (Fig. 6a). Furthermore, highly vesicular clasts (those with >81 vol% vesicles) that require cooling to the phase change temperature to induce sinking can theoretically be deposited hot (that is, at T > 100°C) as a result of the increase in the phase change temperature with water depth (Fig. 6b). For example, at sea level pumice containing 81vol% vesicles will sink at 100°C, whereas at 1000 m water depth (10 MPa) the same pumice will begin to sink at 311˚C. At sea level, dense pumice with a specific gravity of 0.82 (65 vol% vesicles) when first erupted will sink at ~550˚C and at 1000 m water depth the clast will begin to sink at ~600˚C.

Variability in pumice deposition rate will also be controlled by non-uniformity in processes of cooling and water-saturation of pumice. On contact of the hot pumice with seawater, small clasts (lapilli) and the margins of larger clasts (blocks) cool rapidly, whereas the interior of coarser clasts can remain hot, forming a steep within-clast temperature gradient. This gradient is clearly demonstrated in the spacing and intensity of

fractures in pumice clasts deposited on the seafloor. The outer ~1-2 cm margin is intensely cracked and may even show breadcrust texture whereas the interior has more widely spaced incipient fractures (Fig. 5b). Furthermore, water is ingested into the interior of the clast along the most permeable pathways, producing an irregular wet front (e.g., Manville et al., 1998). In addition, cooling of pumice within submarine eruption columns will be influenced by the temperature of the surrounding fluid, which is controlled by the rate of heat transfer from the magmatic ejecta.

Submarine pumice lapilli can therefore be deposited hot if the clasts are erupted at depth, sink quickly (close to the eruption and depositional depth), and ingest heated water. This is not an unrealistic scenario for pumice deposits resulting from the collapse of submarine eruption columns. Would deposition temperatures be sufficient for highly vesicular pumice deposited on the seafloor to thermally weld? Our assessment of an ~300^{o}C maximum depositional temperature for highly vesicular pumice is far lower than that expected for thermal welding in subaerial settings (650-750˚C, Grunder et al., 2005), although the decreased viscosity of the hydrous glass due to the reduced exsolution of water in the magma at high hydrostatic pressures needs also to be considered (e.g., Sparks et al., 1980). However, if the erupted pumice clasts are also relatively dense (<~65 vol% vesicles), then hot deposition, and even welding, may be possible (cf. Kokelaar and Busby, 1992). This leads to the possibility that welding in submarine deposits may be possible in partially water-saturated clasts negating the perceived difficulties of transporting and depositing hot, buoyant gas-filled pumice on the seafloor.

5. Conclusions

Pumice clasts, when first erupted from submarine vents, are hot, filled with magmatic gas (mostly steam), and are buoyant. Our experiments with steam-charged pumice, performed at 1-atm pressure, show that buoyancy is transient as the pumice is quenched in water and becomes water-logged. Moreover, steam-charged pumice need not be super-hot (>400^{o}C) to sink, in contrast to air-filled pumice (Whitham and Sparks, 1986).

Water is first ingested into cooling pumice when steam and other magmatic gases in the vesicles cool and contract. Regardless of the temperature at which pumice begins to

sink, the greatest and most rapid density increase occurs once the clast cools through the steam-liquid water phase transition; this phase change triggers in an abrupt increase in clast settling velocity. Hence, during a submarine eruption, pumice clasts change from being buoyant and hot on eruption, to being negatively buoyant and cooler while mixing with water in the column, at which point they are transported in collapse-generated gravity currents or by water settling. This behaviour contrasts with pumice clasts in subaerial explosive eruptions, which regardless of their temperature, are always more dense than the surrounding air.

Our experiments can be extrapolated to show that the phase change of magmatic steam to liquid water in the vesicles of hot pumice and in the submarine eruption column has an important influence on eruption behaviour and pyroclast dispersal. Condensation of steam causes a rapid change in density and mixing with ambient seawater that promotes collapse. Lapilli and coarse ash, being small, tend to quench rapidly and completely and are therefore likely to be transported in water-supported gravity currents. Larger pumice blocks cool more slowly and may rise to sea level before settling through the water column along with fine ash.

Because the temperature at which pumice becomes saturated and sinks increases with water depth, submarine pumice clasts can be deposited both hot and waterlogged in eruptions sourced in several hundred metres of water and if they cool within the heated water of the eruption column. The resulting deposits, having internal temperatures above that of the surrounding seawater, will be too cool to weld ($\leq 300^{o}$C) unless the pumice clasts are also poorly vesicular (<~65 vol% vesicles).

Our quantitative analysis explains the physical processes accompanying submarine pyroclastic eruptions and demonstrates that they can form primary seafloor pyroclastic deposits, a conclusion reached by others from qualitative studies in ancient terrains now uplifted onto land.

Acknowledgments

We acknowledge the at-sea support provided by the Japan Agency for Marine-Earth Science and Technology (JAMSTEC). We are indebted to the captains, crews, and

operation teams of the RV Kairei and the RV Natsushima, and to Y. Tamura. This research was funded by an ARC Discovery Grant (SRA), the Smithsonian Institution (RSF), and NSF grant EAR 206201 (KVC). Thanks to W. Boykins, T. McCoy, and T. Rose for laboratory help. Reviews by K. Kano, S Mueller, J. White, J. McPhie, N. Riggs and an anonymous reviewer improved a previous version of the manuscript.

References

Allen, S.R., and McPhie, J., 2000. Water-settling and resedimentation of submarine rhyolitic pumice at Yali, eastern Aegean, Greece. J. Volcanol. Geotherm. Res. 95, 285-307.

Bryan, S.E., Cook, A., Evans, J.P., Colls, P.W., Wells, M.G. Lawrence, M.G., Jell, J.S., Greig, A., Leslie, R, 2004. Pumice rafting and faunal dispersion during 2001-2002 in the Southwest Pacific: record of a dacitic submarine explosive eruption from Tonga. Earth Planet. Sci. Lett. 227, 135-154.

Busby-Spera, C.J., 1984. Large volume rhyolite ash-flow eruptions and submarine caldera collapse in the Lower Mesozic Sierra Nevada, California. J. Geophys.Res. 89, 8417-8427.

Busby, C., 2005. Possible distinguishing characteristics of very deepwater explosive and effusive silicic volcanism: Geology, 33, 845-848.

Carslaw, H.S., and Jaeger, J.C., 1959. Conduction of Heat in Solids, 2nd ed. Oxford University Press, Oxford, 510 pp.

Cashman, K.V., Fiske, R.S., 1991. Fallout of pyroclastic debris from submarine volcanic eruptions. Science, 253, 275-280.

De Rosen-Spence, A.F., Provost, G., Dimroth, E., Gochnauer, K., Owen, V., 1980. Archean subaqueous felsic flows, Rouyn-Noranda, Quebec, Canada, and their Quarternary equivalents. Precambr. Res. 12, 43-77.

Dufek, J., Manga, M., and Staedter, M., 2007, Littoral blasts: pumice-water heat transfer and the conditions for steam explosions when pyroclastic flows enter the ocean. J. Geophys. Res. 112 DOI 10.1029/2006JB004910,2007

Fetter, C.W., 1988. Applied Hydrogeology, 2nd Edition; Merrill Publishing Company, Columbus, Ohio.

Fiske, R.S., 1963. Subaqueous pyroclastic flows in the Ohanapecosh Formation, Washington. Geol. Soc. Am. Bull. 74, 391-406.

Fiske, R.S., 1969. Recognition and significance of pumice in marine pyroclastic rocks. Geol. Soc. Am. Bull. 80, 1-8.

Fiske, R.S., Matsuda, T., 1964. Submarine equivalents of ash flows in the Tokiwa Formation, Japan. Am. J. Sci. 262, 76-1061.

Fiske, R.S., Naka, J., Iizasa, K., Yuasa, K., and Klaus, A., 2001. Submarine silicic caldera at the front of the Izu-Bonin arc, Japan: Voluminous seafloor eruptions of rhyolite pumice. Geol Soc. Am. Bull. 113, 813-824.

Grunder. A.L., Laporte, D., and Druitt, T.H., 2005. Experimental and textural investigation of welding: effects of compaction, sintering, and vapor-phase crystallization in the rhyolitic Rattlesnake Tuff. J. Volcanol. Geotherm. Res 142, 89-104.

Head III, J.W., Wilson, L., 2003. Deep submarine pyroclastic eruptions: theory and predicted landforms and deposits, J. Volcanol. Geotherm. Res. 121, 155-193.

660 Hudak, G. J., Morton, R. L., Franklin, J. M, and Peterson, D. M., 2003. Morphology,
661 distribution, and estimated eruption volumes for intracaldera tuffs associated with
662 volcanic-hosted massive sulfide deposits in the Archean Sturgeon Lake Caldera
663 Complex, Northwestern Ontario, *in* White, J., et al., (Eds), Explosive subaqueous
664 volcanism: American Geophysical Union, Geophysical Monograph Series, 140, 345-360.
665 Kato, Y., 1987. Woody pumice generated with submarine eruption: J. Geol. Soc. Japan,
666 93, 11-20.
667
668 Kano, K., 2003. Subaqueous pumice eruptions and their products: A review, *in* J.D.L.
669 White, J.L. Smellie, D.A. Clague (Eds), Explosive subaqueous volcanism. American
670 Geophysical Union, Geophysical Monograph Series, 140, 213-230.
671
672 Kano, K., Yamamoto, T., Ono, K., 1996. Subaqueous eruption and emplacement of the
673 Shinjima Pumice, Shinjima (Moeshima) Island, Kagoshima Bay, SW Japan. J. Volcanol.
674 Geotherm. Res. 71, 187-206.
675
676 Klug, C., Cashman, K.V., 1996. Permeability development in vesiculating magma. Bull.
677 Volcanol. 58, 87-100.
678
679 Kokelaar, P., Busby, C., 1992. Subaqueous explosive eruption and welding of pyroclastic
680 deposits. Science, 257, 196-200.
681
682 McBirney, A.R., 1963. Factors governing the nature of submarine volcanism, Bull.
683 Volcanol. 26, 455-469.
684
685 McPhie, J., Allen, R.L., 2003. Submarine, silicic, syn-eruptive pyroclastic units in the
686 Mount Read volcanics, western Tasmania: Influence of vent setting and proximity on
687 lithofacies characteristics, *in* White, J., et al., (Eds), Explosive subaqueous volcanism:
688 American Geophysical Union, Geophysical Monograph Series, 140, 245-258.
689

690 Manville, V., White, J.D.L., Houghton, B.F., Wilson, C.J.N., 1998. The saturation
691 behaviour of pumice and some sedimentological implications. Sediment. Geol. 119, 5-16.
692
693 Mueller, W., White, J.D.L., 2002. Felsic fire-fountaining beneath Archean seas –
694 pyroclastic deposits of the 2730-Ma Hunter-Mine-Group, Quebec, Canada. J. Volcanol.
695 Geotherm. Res. 54,117-134.
696
697 Murakami, F., Ishihara, T., 1985. Newly discovered submarine calderas in the northern
698 part of the Bonin Arc. Chikyu (Earth) 7, 638-646 (in Japanese).
699
700 Nishimura, A., Marsaglia, K.M., Rodolfo, K.S., Colella, A., Hiscott, R.N., Tazaki, K.,
701 Gill, J.B., Janecek, T., Firth, J., Isiminger-Kelso, M., Herman, Y., Taylor, R.N., Taylor,
702 B., Fujioka, K., 1991. Pliocene-Quaternary submarine pumice deposits in the Sumisu rift
703 area, Izu-Bonin arc, in Fisher RV, Smith GA Sedimentation in volcanic settings: SEPM
704 (Society for Sedimentary Geology) Special Publication, 45, 201-208.
705
706 Reynolds, M.A., Best, J.G., Johnson, R.W., 1980. 1953-57 eruption of Tuluman volcano:
707 rhyolitic volcanic activity in the northern Bismarck Sea. Geol. Surv. Papua New Guinea
708 Mem 7, 44p.
709
710 Rinaldi, M., Campos Venuti, M., 2003. The submarine eruption of the Bombarda
711 volcano, Milos Island, Cyclades, Greece, Bull. Volcanol. 65, 282-293.
712
713 Rust, A.C., Cashman, K.V., 2004. Permeability of vesicular silicic magma: inertial and
714 hysteresis effects. Earth Planet. Sci. Lett. 228, 93-107.
715
716 Simkin, T., Fiske, R.S., 1983. Krakatau 1883- The volcanic eruption and its effects:
717 Smithsonian Institution Press, Washington, 470 p.
718
719 Smithsonian Institution, Home Reef, Bull. Glob. Volcanism Netw. 31 (9) (2006)
720 http://www.volcano.si.edu/

Sparks, R.S.J., Sigurdsson, H., Carey, S.N., 1980. The entrance of pyroclastic flows into the sea, II. theoretical considerations on subaqueous emlacement and welding. J. Volcanol. Geotherm. Res. 7, 97-105.

Stern, R.J., Tamura, Y., Embley, R.W., Ishizuka, O., Merle, S.G., Basu, N.K., Kawabata, H., Bloomer, S.H., 2008. Evolution of West Rota Volcano, an extinct submarine volcano in the southern Mariana Arc: evidence from sea floor morphology, remotely operated vehicle observations and ^{40}Ar-^{39}Ar geochronological studies. Island Arc 17, 70-89.

Stewart, A.L., McPhie, J., 2004. An Upper Pliocene coarse pumice breccia generated by a shallow submarine explosive eruption, Milos, Greece. Bull. Volcanol. 66, 15-28.

Stewart, A.L., McPhie, J., 2006. Facies architecture and Late Pliocene-Pleistocene evolution of a felsic volcanic island, Milos, Greece. Bull. Volcanol. 68, 703-726.

Tani, K., Fiske, R.S., Tamura, Y., Kido, Y., Naka, J., Shukuno, H., Takeuchi, R., 2008. Sumisu volcano, Izu-Bonin arc, Japan: site of a silicic caldera-forming eruption from a small open-ocean island. Bull. Volcanol. DOI 10.1007/200445-007-0153-2

Thomas, R.M.E., Sparks, R.J.S., 1992. Cooling of tephra during fallout from eruption plumes. Bull. Volcanol. 54, 542-553.

Whitham, A., Sparks, R.S.J., 1986. Pumice. Bull. Volcanol. 48, 209-223.

White, J.D.L., 2000. Subaqueous eruption-fed density currents and their deposits Precambr. Res. 101, 87-109.

White, J.D.L., Smellie, J.L., Clague, D.A., 2003. Introduction: a deductive outline and topical overview of subaqueous explosive volcanism. *in*: J.D.L. White, J.L. Smellie, D.A.

751 Clague (Eds), Explosive subaqueous volcanism: American Geophysical Union,
752 Geophysical Monograph Series, 140, 1-23.
753
754 Wilson, L., Sparks, R.S.J., Walker, G.P.L., 1980. Explosive volcanic eruptions –
755 IV. The control of magma properties and conduit geometry on eruption column
756 behaviour, Geophys. J. Roy. Astron. Soc. 63, 117-148.
757
758 Wright, I.C., Gamble, J.A., Shane, P.A.R., 2003. Submarine silicic volcanism of the
759 Healy caldera, southern Kermadec arc (SW Pacific): 1 – volcanology and eruption
760 mechanisms. Bull. Volcanol. 65, 15-29.
761
762 Wright, I.C., Worthington, T.J., Gamble, J.A., 2006. New multibeam mapping and
763 geochemistry of the 30°-35° S sector, and overview, of southern Kermadec arc
764 volcanism: J. Volcanol. Geotherm. Res. 149, 263-296.
765
766 Wright, I.C., Gamble, J.A., 1999. Southern Kermadec submarine caldera arc volcanoes
767 (SW Pacific): Caldera formation by effusion and pyroclastic eruption. Marine Geol. 161,
768 207-227.
769
770 Yuasa, M., Murakami, F., Saito, E., Watanabe, K., 1991. Submarine topography of
771 seamounts on the volcanic front of the Izu-Ogasawara (Bonin) arc. Bull. Geol. Surv.
772 Japan, 42, 703-743.
773
774 Yuasa, M., Kano, K., 2003. Submarine silicic calderas on the northern Shichito-Iwojima
775 Ridge, Izu-Ogasawara (Bonin) Arc, Western Pacific, *in*: J.D.L. White, J.L. Smellie, D.A.
776 Clague (Eds), Explosive subaqueous volcanism, American Geophysical Union,
777 Geophysical Monograph Series, 140, 231-243.
778
779 **FIGURE CAPTIONS**
780

Fig. 1. Measured specific gravities of pumice clasts re-saturated with water compared to measured specific gravities of dry pumice clasts. The expected relationship for fully water-saturated clasts is shown as a dashed line and based on measured solid densities; deviations from this curve are assumed to result from either pore water leakage (low values) or excess water remaining on the clast (high values).

Fig. 2. Experimental data. (a) Examples of the rate of water loss and steam generation during an experimental run at 150°C of three D7 pumice cubes; #13 cube at 30% steam 70% water, #14 cube at 50% steam 50% water, #15 cube at 70% steam 30% water. Filled symbols show the heating track of initially water-saturated cubes to pre-determined ratios of water and steam within the pores; symbols enclosed in squares denote saturation percentages after quenching of water-and-steam-filled clasts in water for 5 minutes. Open symbols show the comparable saturation levels for the same cubes when they had been dried, heated to 150˚C, plunged in water, and weighed after 5 minutes. Shaded domain; pumice sufficiently water-saturated to sink. (b) Resaturation mass of the air-filled control experiments of the three 337-5 (80 vol% vesicles) cubes and three 339-8 (74 vol% vesicles) cubes showing higher degrees of water saturation with increasing temperature.

Fig. 3. Absorption factors after quenching of heated steam-charged pumice cubes (filled circles) and repeated experiments with dry air-filled cubes (open circles; colour identifies the same steam-charged cube). Each dot is the result of a single experiment. (a) D7, 80 vol% vesicles, (b) 337-5, 80 vol% vesicles, (c) 337-1, 73 vol% vesicles, and, (d) 339-8, 73 vol% vesicles. Yellow circles represent dry air-filled experimental runs at both higher and lower temperatures than the steam-filled runs. 70w/30s; represents 70% water, 30% steam. Labeled fields show the degree of absorption anticipated for **contraction** of air alone, **contraction + capillary forces**, and additional saturation due to the **steam**-liquid water phase change.

Fig. 4. Graphs of vesicularity and permeability for samples of submarine erupted and deposited rhyolitic pumice. (a) Connected vesicularity versus total vesicularity for pyroclastic pumice from Yali and Milos, Greece and Sumisu, Izu-Bonin Arc, (crosses),

and quench fragmented pumice from Sumisu (plus signs). Pumice clasts used in the experiments (solid symbols) lie at the high end of the vesicularity spectrum and are dominated by connected vesicles. (b) Permeability vs. total vesicularity for pyroclastic and quench fragmented pumice (as in a). Most samples are highly permeable ($>10^{-13}$ m^2).

Fig. 5. Uplifted submarine erupted and deposited pumice. (a) Elongate vesicular pumice block from Yali, Greece. (b) Internally fractured pumice block with a quenched margin from Milos, Greece. (c) Weakly stratified pumice lapilli from Yali, Greece. (d) Reversely graded pumice from Milos, Greece. Lower part; weakly stratified pumice lapilli, upper part; water-settled pumice blocks and ash. Scale bar, 5 m.

Fig. 6. Theoretical cooling and specific gravity trajectories of submarine-erupted pumice clasts. (a) Calculated trajectories show saturation paths for pumice clasts of different vesicularities; the temperature at which pumice is sufficiently water-saturated to sink (shaded region) decreases as the initial clast vesicularity increases. (b) Calculated cooling and density trajectories for highly vesicular pumice (81 vol% vesicles) as a function of initial water depth; saturation temperature increases with increasing water depth because of changes in the temperature of the steam-to-liquid water phase transition.

Fig. 7. Schematic cartoon of the saturation front required to allow pumice clasts with variable initial vesicularities (60, 77 and 85 vol%) to sink.

Table 1 Location and properties of the pumice blocks.

Sample	latitude (N)	longitude (E)	sample depth (m)	max length (cm)	variation in specific gravity (kg/m^3) theoretical	saturated	dry	porosity^ vol% total	isolated
D7*	30.2833	139.1833	1348-700	23	1.25±0.01	1.25±0.05	0.45±0.03	80.5	2.0
337-1#	31.6188	139.7227	1466	31	1.32±0.03	1.33±0.07	0.6±0.03	72.6	2.4
337-5#	31.6187	139.7240	1343	35	1.24±0.02	1.24±0.02	0.44±0.03	80.2	3.0
339-8#	31.5391	139.8369	323	46	1.33±0.03	1.33±0.06	0.63±0.08	73.8	1.7

*dredge, #ROV, ^He pycnometer measurements

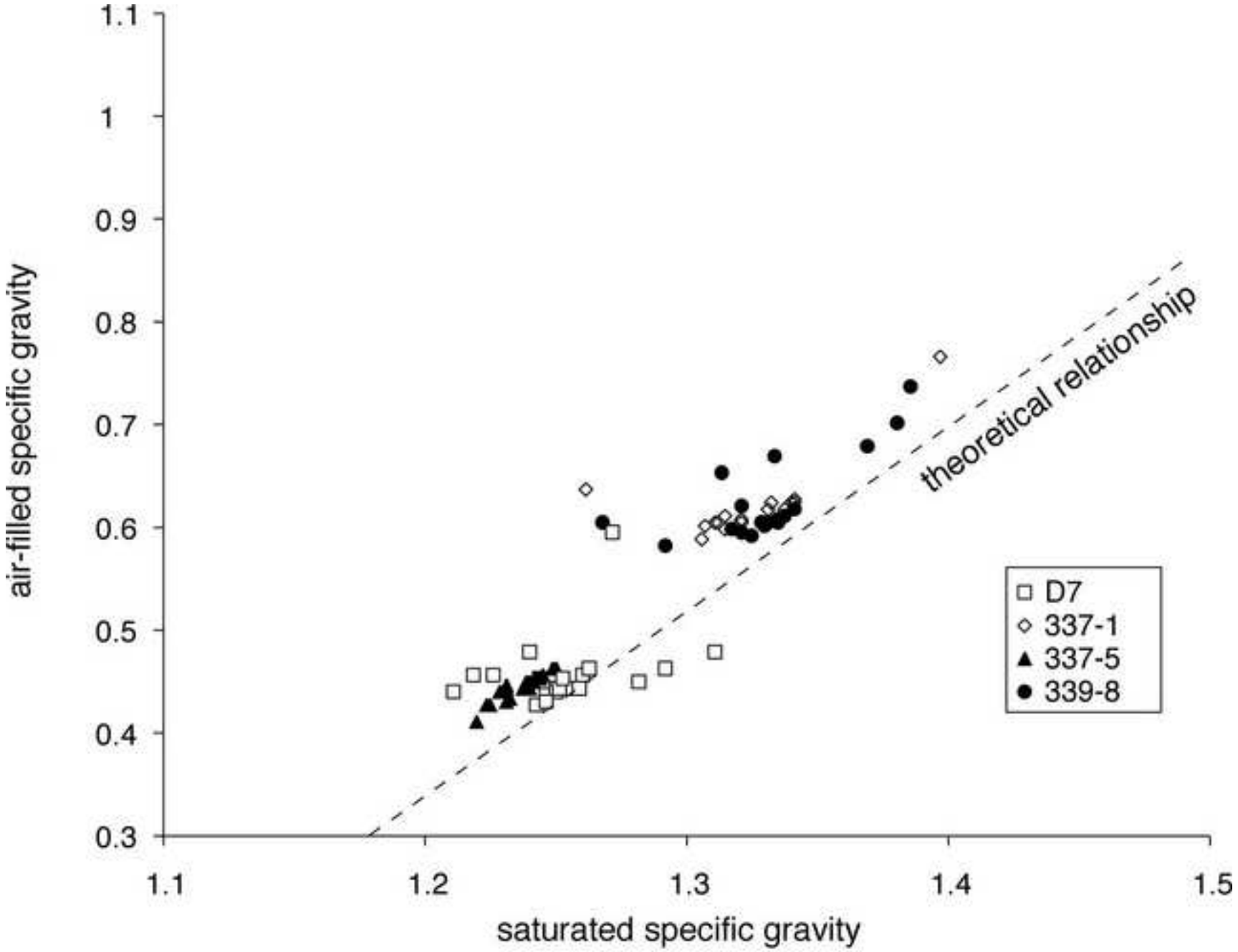

Figure 1

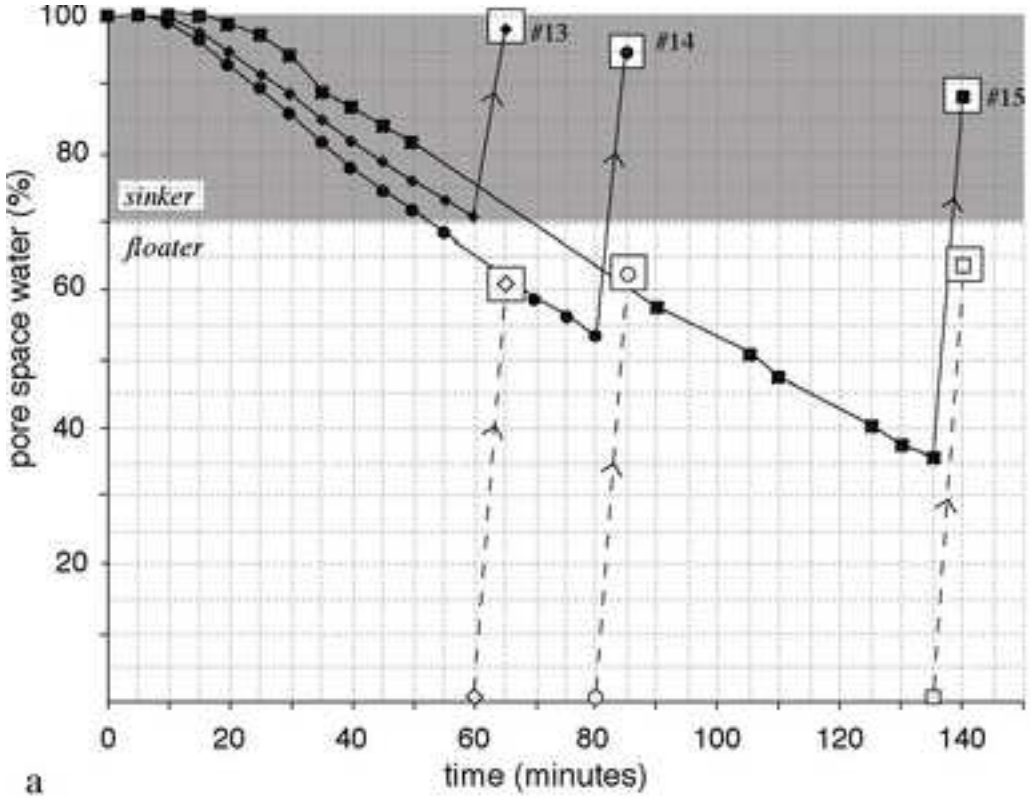

a

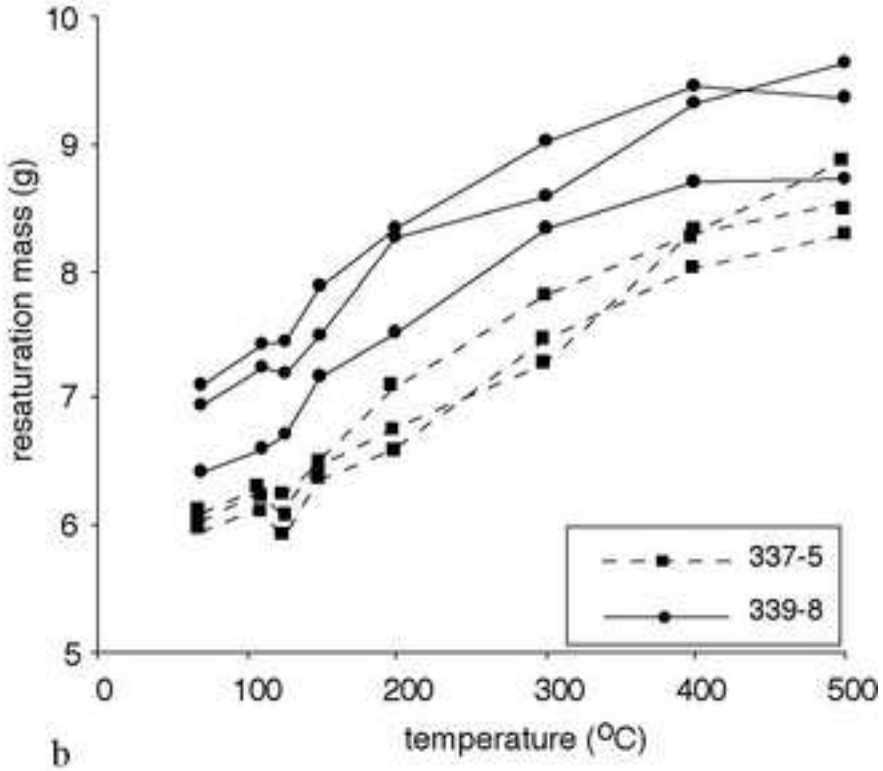

b

Figure 2

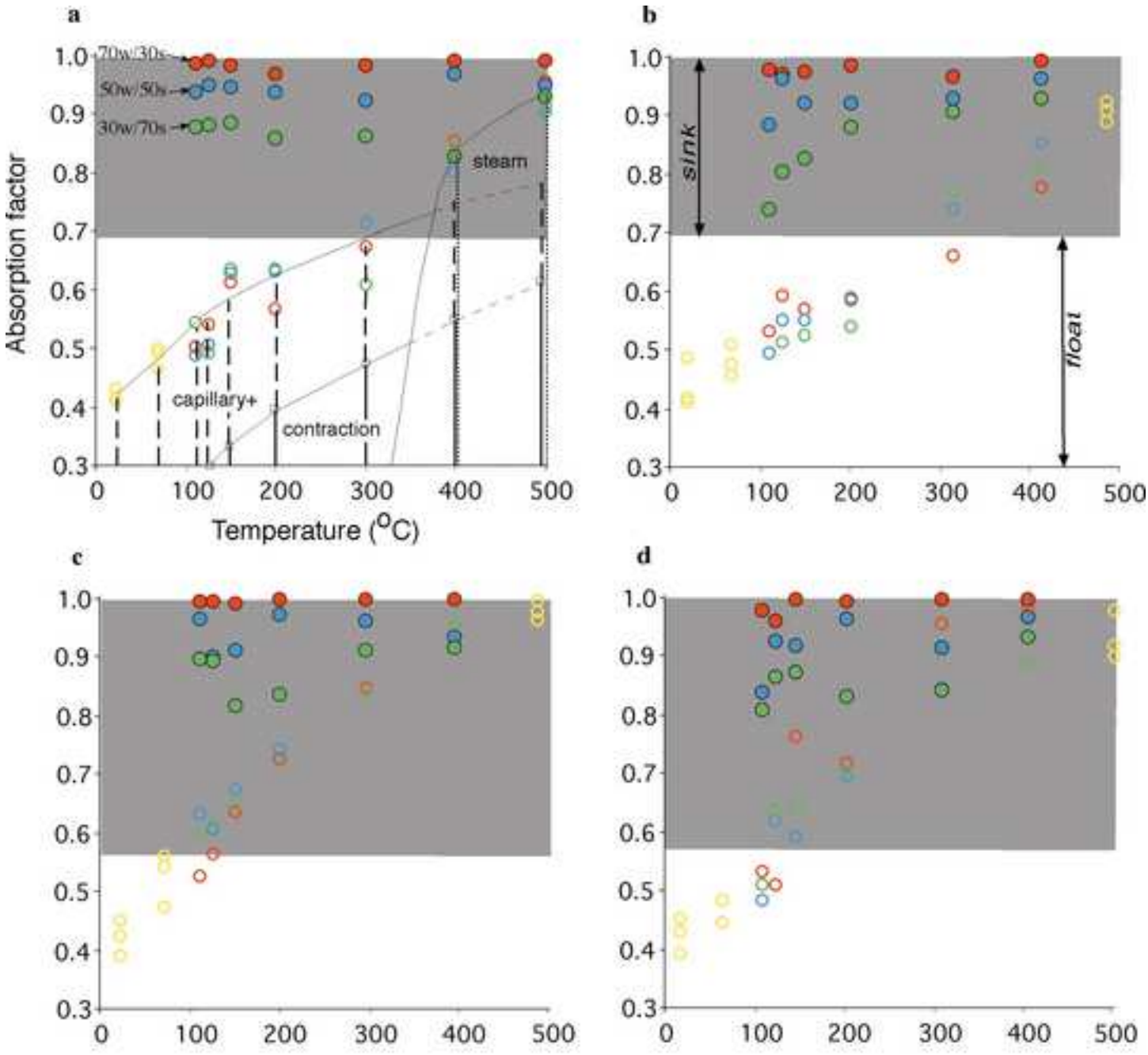

Figure 3

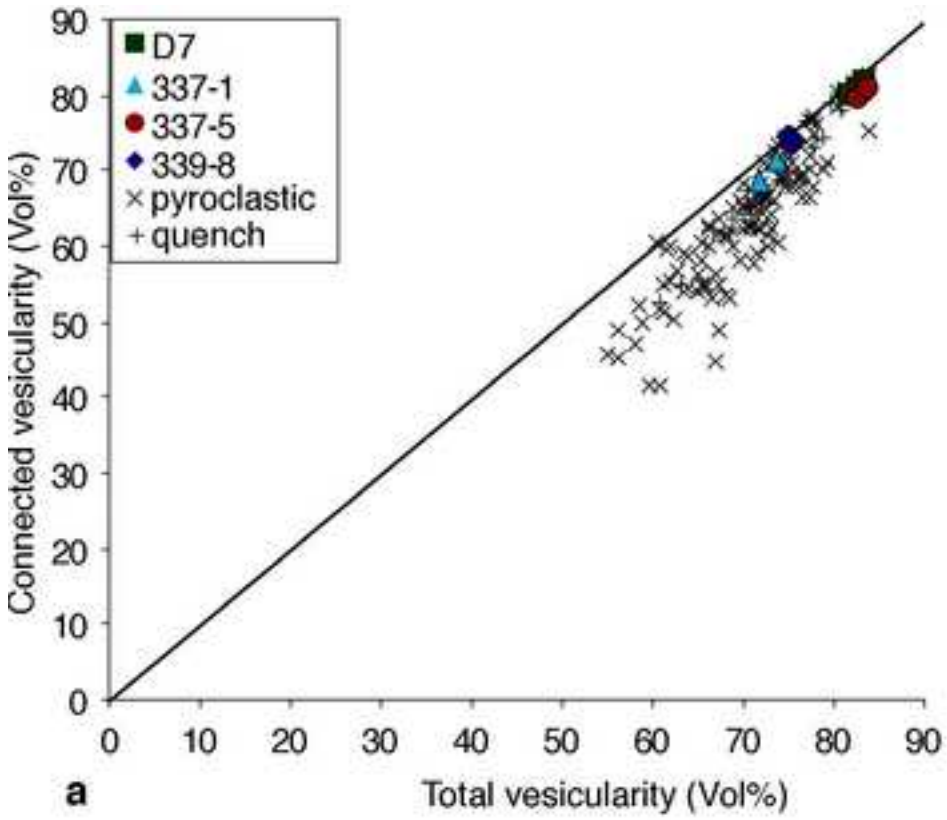

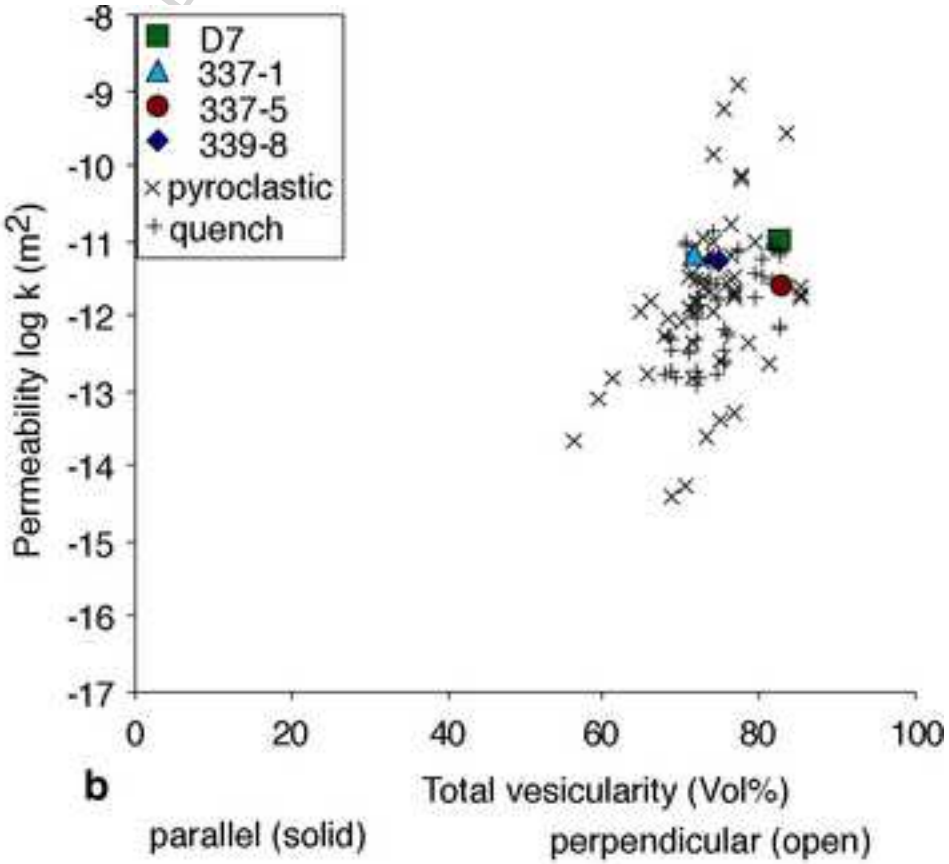

Figure 4

a

b

c

d

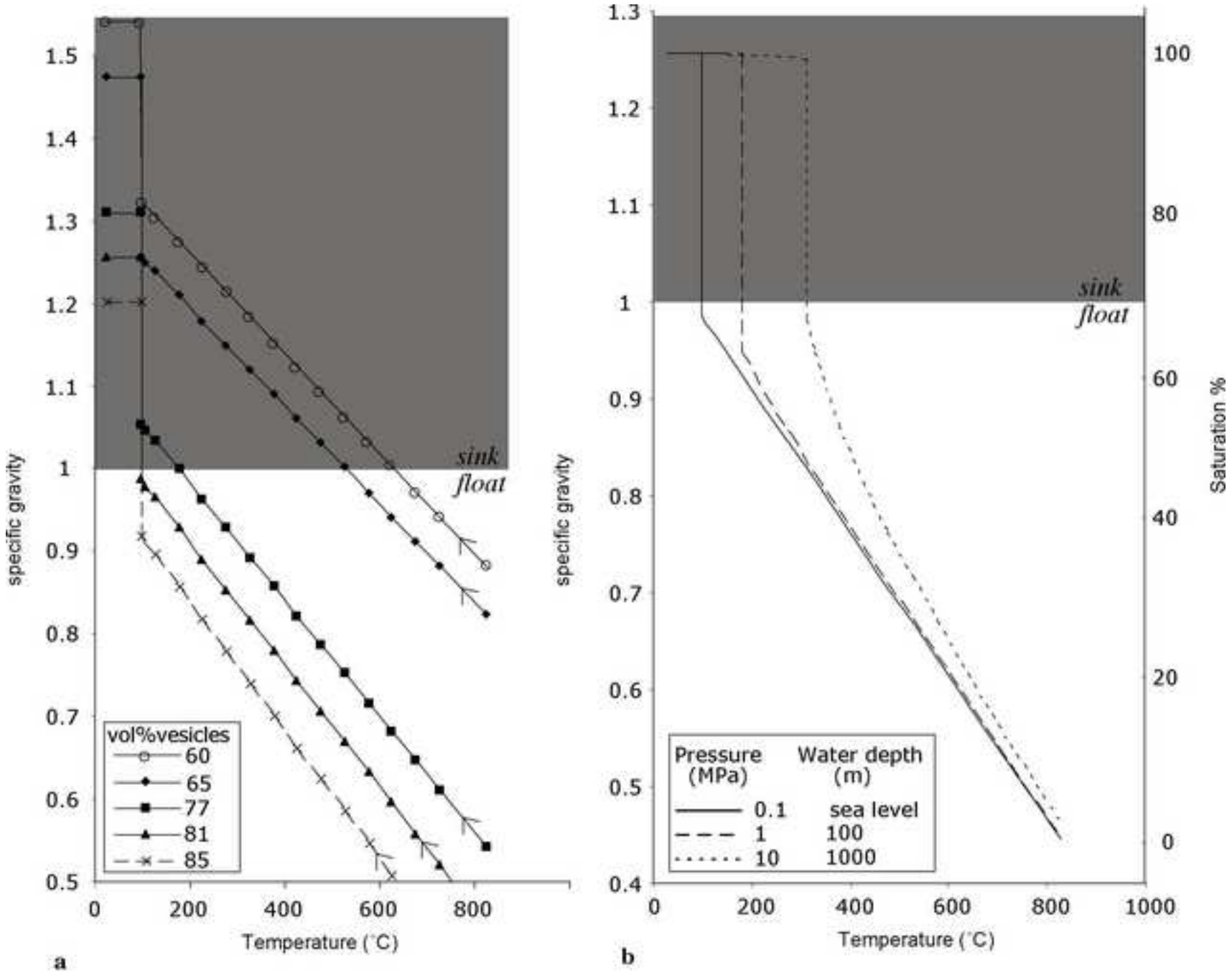

Figure 6

Figure 7